Time-Resolved X-Ray Diffraction from Coherent Phonons during a Laser-Induced Phase Transition

A. M. Lindenberg,[1] I. Kang,[1] S. L. Johnson,[1] T. Missalla,[2,5] P. A. Heimann,[2] Z. Chang,[3] J. Larsson,[4] P. H. Bucksbaum,[3] H. C. Kapteyn,[3] H. A. Padmore,[2] R. W. Lee,[5] J. S. Wark,[6] and R. W. Falcone[1,7]

[1]*Department of Physics, University of California, Berkeley, California 94720*
[2]*Advanced Light Source, Lawrence Berkeley National Laboratory, Berkeley, California 94720*
[3]*Center for Ultrafast Optical Science, University of Michigan, Ann Arbor, Michigan 48109*
[4]*Atomic Physics Division, Lund Institute of Technology, Lund, Sweden*
[5]*Lawrence Livermore National Laboratory, Livermore, California 94551*
[6]*Department of Physics, Clarendon Laboratory, University of Oxford, Oxford OX1 3PU, United Kingdom*
[7]*Center for Beam Physics, Lawrence Berkeley National Laboratory, Berkeley, California 94720*

(Received 17 August 1999)

Time-resolved x-ray diffraction with picosecond temporal resolution is used to observe scattering from impulsively generated coherent acoustic phonons in laser-excited InSb crystals. The observed frequencies and damping rates are in agreement with a model based on dynamical diffraction theory coupled to analytic solutions for the laser-induced strain profile. The results are consistent with a 12 ps thermal electron-acoustic phonon coupling time together with an instantaneous component from the deformation-potential interaction. Above a critical laser fluence, we show that the first step in the transition to a disordered state is the excitation of large amplitude, coherent atomic motion.

PACS numbers: 63.20.Kr, 61.10.–i, 64.70.Dv, 78.47.+p

Recent developments in time-resolved x-ray diffraction, using both synchrotron and laser-plasma based sources, have led to the capability of directly observing structural phase transitions, the motion of complex molecules, and chemical reactions, on picosecond time scales. This has resulted in a number of novel experiments, including the investigation of short-pulse-laser irradiation of organic films and ultrafast laser-induced phase transitions in semiconductors [1–3]. In experiments of relevance to biology, real-time studies of photoinitiated reactions in molecules such as myoglobin and photoactive yellow protein (PYP) have been performed [4,5]. Recent experiments utilizing a laser-produced Cu $K\alpha$ source have demonstrated x-ray diffraction from a coherent acoustic pulse induced by laser heating of GaAs [6]; however, while diffraction from expanded and compressed regions of the crystal were observed, no temporal oscillations in the x-ray intensity at the relevant phonon frequencies were recorded.

In this Letter we report the direct observation of x-ray diffraction from laser-induced coherent acoustic phonons at frequencies up to 0.1 THz. The results are in quantitative agreement with simulations based on dynamical diffraction theory, and consistent with an interpretation based on the excitation of coherent phonon states. Moreover, for sufficiently high laser fluences, we observe a reversible, optically induced phase transition which develops on a time scale equal to one-half of a phonon period. We thus show that the approach to disorder is through the excitation of large-amplitude, coherent lattice motion.

The experimental setup is similar to previous experiments [2,7]. A bending magnet beam line at the Advanced Light Source synchrotron produces light in a broad spectrum up to photon energies of ~10 keV. A Si (111) monochromator crystal selects a single wavelength of 2.4 Å with a spectral bandwidth of 1 mÅ. The diffracted beam is then directed onto an InSb crystal oriented near the Bragg angle for the (111) reflection. To better match the penetration depths of the laser and x rays, the crystal is asymmetrically cut so that the diffracted beam leaves the crystal at a grazing angle of 3°. We use a Ti:Al_2O_3-based 150 fs, 1 kHz, 800 nm laser, synchronized to the individual electron bunches within the synchrotron ring with jitter less than 5 ps. The laser is incident on the InSb crystal and overlapped in both space and time with a single x-ray pulse. The time-resolved x-ray diffracted intensity following laser excitation is then measured using a streak camera detector triggered by a GaAs photoconductive switch [8]. A CCD camera records the x-ray streak projected onto a phosphor screen. All recorded data are averaged for a period of about 1 min which corresponds to 60 000 shots. The resulting temporal resolution of the camera is 3 ps; this is monitored using an ultraviolet femtosecond pulse split off from the main pump laser. The entire time history of the diffracted signal following laser excitation is measured at once, in contrast to more typical pump-probe geometries.

Coherent phonons are manifested as oscillatory signals in time-resolved x-ray diffraction. As an example, Fig. 1(a) shows an unperturbed, diffracted x-ray pulse measured at 40 arc sec from the Bragg peak, together with one for which the laser is incident on the crystal during the pulse. At a fluence 20% below the damage threshold of 15 mJ/cm^2 (defined as the fluence resulting in a permanent decrease in the diffracted intensity within a few seconds), the laser modifies the diffraction efficiency of the crystal and induces temporal structure within the

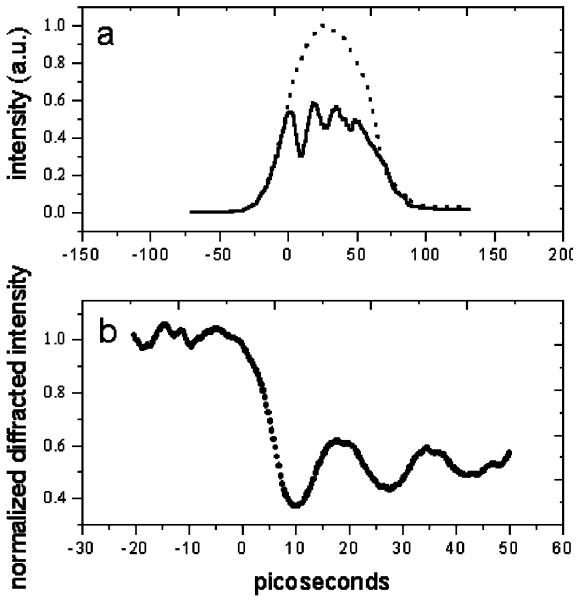

FIG. 1. (a) Unperturbed (dashed line) and laser-perturbed (solid line) diffracted x-ray pulses measured at an angle of +40 arc sec from the Bragg peak. (b) Normalized time-resolved diffracted intensity derived from (a).

diffracted x-ray pulse. The normalized diffracted intensity is determined by dividing the laser-perturbed x-ray pulse by the unperturbed pulse, as shown in Fig. 1(b). At this angle, following an initial drop in the diffracted intensity that results from a shift of the Bragg peak, distinct temporal oscillations are observed with a period of about 20 ps, indicative of large-amplitude, coherent lattice oscillations.

Impulsive excitation of a solid on a time scale shorter than the material's hydrodynamic response time generates coherent acoustic phonons across a range of wave vectors near the Brillouin zone center and peaked at a wave vector of order one inverse laser penetration depth. A phonon of wave vector **q** induces an extra time-dependent periodicity to the lattice. This gives rise to sidebands centered on the Bragg peak, exactly as in the case of x-ray diffuse scattering [9], a technique normally used as a probe of incoherent phonon distributions. In our experiment, since the phonons are coherently excited, the sidebands oscillate at the phonon frequency and we directly resolve this coherent time-dependent atomic motion. Diffraction from transducer-excited MHz ultrasonic waves has been observed previously [10,11].

By wave vector matching considerations, the oscillation frequency ω for a deviation $\Delta\theta$ from the Bragg angle θ for a symmetric reflection from the plane with reciprocal lattice vector **G** is given by

$$\omega = v|\mathbf{G}|\Delta\theta \cot\theta , \qquad (1)$$

where v is the speed of sound within the crystal. This result can also be derived directly from dynamical diffraction theory by considering the time and angle dependence of the rocking curve fringes of a crystal whose thickness increases at the sound speed. Thus, as the crystal angle is varied, different phonon modes are selected out of the broad spectrum of excited modes. By measuring the oscillation frequency as a function of crystal angle, the acoustic phonon dispersion relation is mapped out near the Brillouin zone center, as shown in Fig. 2, with slope proportional to the sound velocity in the crystal. To quantify this, taking into account the effects of x-ray absorption and extinction, we note that the superposition of excited coherent phonon modes corresponds to a certain time and spatially dependent strain profile, as derived by Thomsen *et al.* [12] (see inset, Fig. 2). The Tagaki-Taupin [13,14] equations for the dynamical diffraction of x rays are solved for different values of the sound velocity, assuming one-dimensional strain propagation along the [111] direction. We extract a sound velocity of ~4000 m/s, in agreement with the known value for InSb (3900 m/s) [15]. No indication of softening or anharmonicity in the LA phonon mode is observed.

There are two mechanisms that provide for the initial excitation of coherent acoustic phonons. For the case of femtosecond optical excitation of polar semiconductors, heating of the lattice is thought to occur through the initial excitation of hot carriers, their subsequent relaxation to the band edge through LO-phonon emission, and a further decay into an acoustic phonon cascade, a pathway which is thought to take ~10 ps to complete [3]. The increase in lattice temperature over this time scale stresses the material, which then relaxes through a strain wave propagating at the sound velocity deeper into the material. On the other hand, more direct coupling from hot carriers to acoustic phonons is provided through the acoustic deformation potential [16], in which the stress, provided by a carrier-induced change in the crystalline potential, is effectively instantaneous.

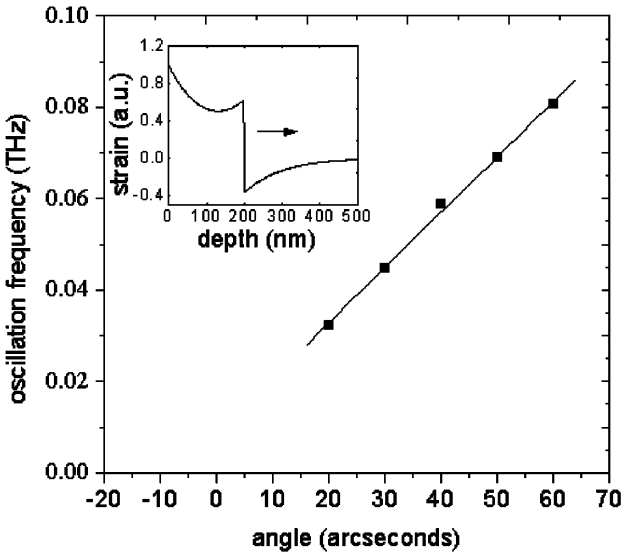

FIG. 2. Experimentally observed oscillation frequency of the diffracted intensity as a function of crystal angle. The solid line is a fit to the data. Inset: Calculated laser-induced strain profile, which propagates at the sound velocity into the material.

Assuming that the electrons and phonons maintain separate states of equilibrium characterized by temperature deviations δT_e and δT_p, the combined stress due to these two effects can be written as [17,18]

$$\sigma \sim \gamma_e C_e \delta T_e + \gamma_p C_p \delta T_p , \quad (2)$$

where C_e and C_p are the specific heats of the electrons and the ions, and γ_e and γ_p are the corresponding Grüneisen factors for the electron and phonon subsystems. While the thermal contribution to the stress is dominant after electron-lattice equilibration, the electronic term scales as nT_e^2 [18], where n is the carrier density, so that the initial hot, dense carrier distribution ($T_e \geq 1$ eV, $n \geq 10^{21}$ cm^{-3}) implies a significant electronic contribution to the impulsively driven lattice at short times.

For an instantaneously heated crystal with an exponential temperature profile near the surface, the associated time-dependent stress and strain profiles have been derived by Thomsen *et al.* [12]. However, in accordance with the above discussion, we find that in order to obtain agreement between our model and the observed temporal behavior, it is necessary to modify the profile of the acoustic pulse to take into account the effect of a finite electron-acoustic phonon coupling time. We note that this has no effect on the determination of the dispersion relation in Fig. 2. The elastic equations in a continuum model are solved assuming a slowly developing stress representing the indirect electron-acoustic phonon coupling time, and an instantaneous stress from the deformation potential. The slow term blurs the sharp boundary between the expansive and compressive components of the Thomsen strain profile [17] and reduces the modulation depth of the oscillations. The fast term generates coherent phonons on time scales faster than the thermal coupling time which otherwise would not be coherent.

Figure 3 shows the time-dependent diffracted intensity measured at 0, +20, and +40 arc sec from the Bragg peak, along with the calculated (normalized) diffracted intensity at each angle. There are three adjustable parameters in the model: the electron-acoustic phonon coupling time and the amplitudes of the thermal and deformation-potential generated stress. A single set of parameters matches all experimental curves. Best fit corresponds to a coupling time of 12 ± 3 ps (in agreement with previous results [3]), and a thermal strain of 0.17% ± 0.03% (just below that of InSb at its melting temperature), together with a nonthermal contribution of 0.08% ± 0.03%, about a factor of 2 smaller. We note that the first 10 ps cannot be modeled without inclusion of an instantaneous term while the long-time behavior cannot be modeled without a slower developing term of order 10 ps. Inclusion of thermal diffusion following Ref. [12] has negligible effect on the time scales discussed in this paper; more rapid carrier diffusion on time scales faster than the electron-phonon coupling time will effectively increase the region in which the laser energy is deposited. However, we obtain good fits to the data using the tabulated laser penetration depth (100 nm),

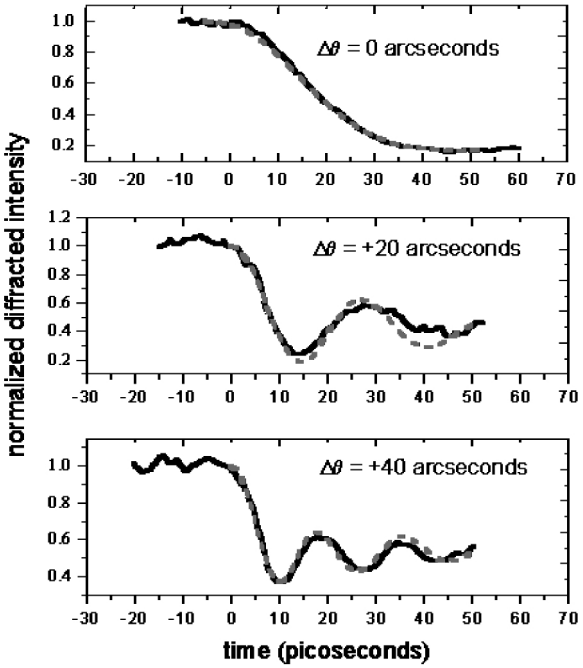

FIG. 3. Experimentally measured (solid line) and simulated (dashed line) time-resolved diffracted intensity at crystal angles of 0, +20, and +40 arc sec from the Bragg peak.

so do not expect this to be a significant effect. The damping of the oscillations over 50 ps is due to the spectral bandwidth set by the Si monochromator crystal and is included in our model by averaging over the Si rocking curve width; this is the time scale for the finite range of phonons probed at each crystal angle to dephase.

The observed oscillation amplitude can be used to estimate the amplitude of a single phonon mode [19]. We obtain a peak value of ~10% of the lattice spacing. The slow heating of a solid to its melting temperature is often interpreted in terms of the Lindemann melting criterion [20], in which a first order transition from an ordered to a disordered state occurs when atomic vibrational amplitudes approach a critical value equal to ~10% of the lattice spacing. Lattice dynamical calculations show that at the melting temperature of InSb the incoherent acoustic phonon root-mean-square amplitude is indeed of this order [21]. At a laser fluence just below melting threshold, we thus observe coherent acoustic phonons corresponding in amplitude to the incoherent phonons one would expect from InSb near its melting point.

In the regime discussed above, the laser-induced state is thus characterized by a maximally strained lattice undergoing large-amplitude oscillations about the equilibrium lattice positions. At a slightly higher laser fluence, 10% below the damage threshold, no coherent oscillations occur, as shown in Fig. 4. On the Bragg peak, a 60% reduction in the diffracted intensity occurs over ~20 ps. At +60 arc sec from the Bragg maximum, a 40% reduction in intensity (smaller due to the larger x-ray penetration depth off the Bragg peak) occurs on a time scale limited by the

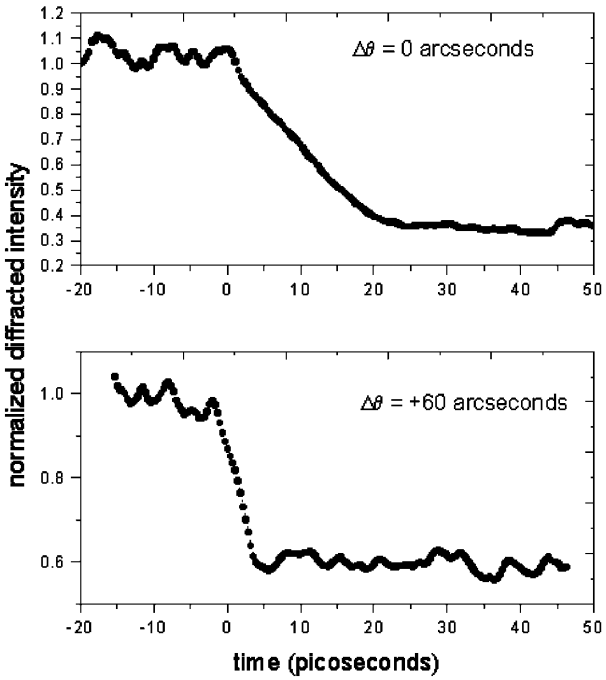

FIG. 4. Time-resolved diffracted intensity at 0 and +60 arc sec from the Bragg peak near the laser damage threshold. At 60 arc sec, the diffracted intensity falls within 3 ps.

streak camera temporal resolution (3 ps). At angles between the Bragg peak and +60 arc sec, a continuum of decay times is observed, with the time scale of the decay decreasing as the crystal is tuned further from the Bragg angle. In effect, above a critical fluence, only the first half period of the oscillations that were induced at lower fluences are observed.

We interpret these findings as follows. At low fluences, impulsive excitation of the solid induces small-amplitude, coherent atomic motion about equilibrium lattice positions. Above a critical fluence of 13 mJ/cm^2, the lattice no longer coherently oscillates about this equilibrium value, but instead is coherently driven into a disordered state. This occurs on a time scale set by one-half of a phonon period, at which point the average atomic displacement is maximum for a given mode, in analogy with the Lindemann criterion. Since the diffracted x-ray intensity does not oscillate, this is indicative of a state for which atomic motion with long-range coherence does not exist. In other words, loss of coherence on fast time scales is an indication of disorder on fast time scales.

As the crystal angle is varied relative to the Bragg peak, phonons of differing wave vectors **q** are probed; equivalently, different length scales are being probed. Thus disorder develops over shorter length scales (large **q**) in less time than longer length scales (small **q**). One may observe a change in the diffracted intensity on arbitrarily fast time scales by tuning the crystal angle sufficiently far from the Bragg peak, presumably limited by the time scale on which the lattice stress develops. Since the observed 3 ps drop in the diffracted intensity occurs faster than the thermal coupling time (without the delay observed in Ref. [3]), we conclude that the first step in the observed disordering transition at high laser fluence is the initial excitation of hot carriers which subsequently drive large-amplitude, coherent vibrational motion, a transition essentially nonthermal in nature [22].

In conclusion, we have shown that time-resolved x-ray diffraction is a useful tool in phonon spectroscopy and a sensitive probe of electron-phonon coupling strengths. For low laser fluences we measure oscillations in the x-ray diffraction efficiency corresponding to coherent phonons at frequencies up to 0.1 THz. At higher fluences a reversible phase transition has been observed, driven by large amplitude, correlated atomic motion, the first step in the approach towards disorder.

This work was supported by the Department of Energy through the High Energy Density Science Grants Program, ILSA at Lawrence Livermore National Laboratory, Lawrence Berkeley National Laboratory, and the National Science Foundation.

[1] C. Rischel *et al.*, Nature (London) **390**, 490 (1997).
[2] J. Larsson *et al.*, Appl. Phys. A **66**, 587 (1998).
[3] A. H. Chin *et al.*, Phys. Rev. Lett. **83**, 336 (1999).
[4] V. Srajer *et al.*, Science **274**, 1726 (1996).
[5] B. Perman *et al.*, Science **279**, 1946 (1998).
[6] C. Rose-Petruck *et al.*, Nature (London) **398**, 310 (1999).
[7] J. Larsson *et al.*, Opt. Lett. **22**, 1012 (1997).
[8] Z. Chang *et al.*, Appl. Phys. Lett. **69**, 133 (1996).
[9] E. H. Jacobsen, Phys. Rev. **97**, 654 (1954).
[10] L. D. Chapman, R. Colella, and R. Bray, Phys. Rev. B **27**, 2264 (1983).
[11] K. D. Liss *et al.*, Proc. SPIE Int. Soc. Opt. Eng. **3451**, 117 (1998).
[12] C. Thomsen, H. T. Grahn, H. J. Maris, and J. Tauc, Phys. Rev. B **34**, 4129 (1986).
[13] S. Takagi, Acta Crystallogr. **15**, 1311 (1962).
[14] J. Burgeat and D. Taupin, Acta Crystallogr. A **24**, 99 (1968).
[15] *Semiconductors—Basic Data*, edited by O. Madelung (Springer-Verlag, Berlin, Heidelberg, 1996), p. 147.
[16] J. J. Baumberg, D. A. Williams, and K. Kohler, Phys. Rev. Lett. **78**, 3358 (1996).
[17] O. B. Wright, Phys. Rev. B **49**, 9985 (1994).
[18] M. Nisoli *et al.*, Phys. Rev. B **55**, R13 424 (1997).
[19] P. H. Bucksbaum and R. Merlin, Solid State Commun. (to be published).
[20] F. A. Lindemann, Z. Phys. **11**, 609 (1910).
[21] J. F. Vetelino and S. P. Gaur, Phys. Rev. B **5**, 2360 (1972).
[22] K. Sokolowski-Tinten *et al.*, Phys Rev. B **58**, R11 805 (1998).